4-22-2011

Effect of the Ionic Conductivity of the Electrolyte in Composite SOFC Cathodes

Rainer Küngas
University of Pennsylvania, kungas@seas.upenn.edu

John M. Vohs
University of Pennsylvania, vohs@seas.upenn.edu

Raymond J. Gorte
University of Pennsylvania, gorte@seas.upenn.edu

Suggested Citation:
Küngas, R., Vohs, J.M. and Gorte, R.J. (2011). Effect of the Ionic Conductivity of the Electrolyte in Composite SOFC Cathodes. *Journal of the Electrochemical Society,* **158** (6) B743-B748.

Effect of the Ionic Conductivity of the Electrolyte in Composite SOFC Cathodes

Abstract

Solid oxide fuel cell (SOFC) cathodes were prepared by infiltration of 35 wt % $La_{0.8}Sr_{0.2}FeO_3$ (LSF) into porous scaffolds of three, zirconia-based electrolytes in order to determine the effect of the ionic conductivity of the electrolyte material on cathode impedances. The electrolyte scaffolds were 10 mol % Sc_2O_3-stabilized zirconia (ScSZ), 8 mol % Y_2O_3-stabilized zirconia (YSZ), and 3 mol % Y_2O_3- 20 mol % Al_2O_3-doped zirconia (YAZ), prepared by tape casting with graphite pore formers. Each electrolyte scaffold was 65% porous, with identical pore structures as determined by scanning electron microscopy (SEM). Both symmetric cells and fuel cells were prepared and tested between 873 and 1073 K, using LSF composites that had been calcined to 1123 or 1373 K. Literature values for the electrolyte conductivities were confirmed using the ohmic losses from the impedance spectra. The electrode impedances decreased with increasing electrolyte conductivity, with the dependence being between to the power of 0.5 and 1.0, depending on the operating temperature and LSF calcination temperature.

Disciplines

Biochemical and Biomolecular Engineering | Chemical Engineering | Engineering

Comments

Suggested Citation:
Küngas, R., Vohs, J.M. and Gorte, R.J. (2011). Effect of the Ionic Conductivity of the Electrolyte in Composite SOFC Cathodes. *Journal of the Electrochemical Society,* **158** (6) B743-B748.

Journal of The Electrochemical Society, **158** (6) B743-B748 (2011)
0013-4651/2011/158(6)/B743/6/$28.00 © The Electrochemical Society

Effect of the Ionic Conductivity of the Electrolyte in Composite SOFC Cathodes

Rainer Küngas,[*] John M. Vohs,[**] and Raymond J. Gorte[,z]**

Department of Chemical and Biomolecular Engineering, University of Pennsylvania, Philadelphia, Pennsylvania 19104, USA

Solid oxide fuel cell (SOFC) cathodes were prepared by infiltration of 35 wt % $La_{0.8}Sr_{0.2}FeO_3$ (LSF) into porous scaffolds of three, zirconia-based electrolytes in order to determine the effect of the ionic conductivity of the electrolyte material on cathode impedances. The electrolyte scaffolds were 10 mol % Sc_2O_3-stabilized zirconia (ScSZ), 8 mol % Y_2O_3-stabilized zirconia (YSZ), and 3 mol % Y_2O_3- 20 mol % Al_2O_3-doped zirconia (YAZ), prepared by tape casting with graphite pore formers. Each electrolyte scaffold was 65% porous, with identical pore structures as determined by scanning electron microscopy (SEM). Both symmetric cells and fuel cells were prepared and tested between 873 and 1073 K, using LSF composites that had been calcined to 1123 or 1373 K. Literature values for the electrolyte conductivities were confirmed using the ohmic losses from the impedance spectra. The electrode impedances decreased with increasing electrolyte conductivity, with the dependence being between to the power of 0.5 and 1.0, depending on the operating temperature and LSF calcination temperature.
 [DOI: 10.1149/1.3581109]

Manuscript submitted November 17, 2010; revised manuscript received January 27, 2011. Published April 22, 2011. This was Paper 840 presented at the Montreal, QC, Canada, Meeting of the Society, May 1–6, 2011.

The performance of solid oxide fuel cells (SOFCs) is often limited by the slow kinetics of the oxygen reduction reaction at the cathode. The ideal SOFC cathode material would have excellent catalytic activity, together with high electronic conductivity (to provide electrons for the oxygen reduction reaction) and ionic conductivity (to transport the oxygen ions from the cathode into the electrolyte)[1–3] The material most commonly used in SOFC cathodes is LSM ($La_{1-x}Sr_xMnO_3$), which satisfies the conditions of catalytic activity and electronic conductivity, but has a very low ionic conductivity (4×10^{-8} S/cm at 1073 K).[4] When pure LSM is used as the cathode, its low ionic conductivity results in the active zone of the cathode being limited to the three-phase boundary (TPB) line in the immediate vicinity of the electrolyte. In order to extend the reaction zone further into the cathode bulk, LSM is usually mixed with a good ionic conductor, most commonly the electrolyte material (e.g. YSZ, yttria-stabilized zirconia) to form a composite.[3,5–12] Such composites combine the best of the properties of both components, resulting in a material that simultaneously meets all the requirements for SOFC cathodes. In addition to providing more TPB sites, the use of composites is also advantageous for mechanical stability, since it alleviates the problem of thermal expansion coefficient mismatch between the electrolyte and electronic conductor.[13–15]

Alternative perovskites with mixed ionic and electronic conductivity (MIEC), such as LSF ($La_{1-x}Sr_xFeO_3$) or LSCF ($La_{1-x}Sr_xCo_{1-y}Fe_yO_3$) have also been proposed as cathode materials for SOFCs, especially for operation at lower temperatures, 873–1073 K.[16–25] The ionic conductivity of LSF is significantly higher than that of LSM (8.3×10^{-4} S/cm at 973 K),[26] so that oxygen adsorption and reduction do not have to be spatially confined to the TPB sites.[3,15,27] However, the ionic conductivity of MIECs is still much lower than that of the YSZ (1.8×10^{-2} S/cm at 973 K).[28] Therefore, using a composite of an MIEC perovskite and YSZ can significantly improve the performance of SOFC cathodes compared to using the perovskite alone.

The motivation of the present study was to better understand the effect of the ionic conductivity of the electrolyte in composite cathodes. Although numerous studies, both experimental and theoretical, suggest that the ionic conductivity of the electrolyte within composite SOFC electrodes can be very important for electrode performance, we are unaware of any systematic investigations on this topic. For example, while it has been demonstrated that the substitution of YSZ in Ni-YSZ anodes with doped ceria results in performance enhancement,[29–32] it remains uncertain whether this is due to the higher ionic conductivity of ceria or to the fact that ceria possesses significant catalytic activity for the electrode reaction. That catalytic activity may be responsible is suggested from the results of Sumi, et al. who compared the performance of Ni-YSZ and Ni-ScSZ (scandia-doped zirconia) anodes.[33] While the ionic conductivity of ScSZ is significantly higher than that of YSZ, the authors found negligible differences in performance for Ni-YSZ and Ni-ScSZ electrodes, with YSZ-based cells even outperforming the ScSZ-cells under some conditions.[33]

The situation is similarly uncertain for SOFC composite cathodes. Perry Murray and Barnett observed significantly lower polarization resistances for composites of LSM with Gd-doped ceria compared to that of LSM-YSZ (Ref. 34) and Yamahara et al. reported improved performance of LSM-SYSZ [$SYSZ = (Sc_2O_3)_{0.1}(Y_2O_3)_{0.01}(ZrO_2)_{0.89}$] electrodes compared to LSM-YSZ due to the higher ionic conductivity of SYSZ,[35] However, Wang et al. reported that the polarization resistance of LSM-ScCeSZ (scandia-ceria stabilized zirconia) composite cathodes decreased with ceria content, in the direction opposite to increasing ionic conductivity.[36] Finally, modeling studies by Tanner et al.,[3] and Bidrawn et al.[37] suggest that the polarization resistance of composite electrodes should have an inverse square-root dependence on the ionic conductivity of the electrolyte, provided all other parameters are held constant.

Unfortunately, it is very difficult to ensure that only one parameter is varied at a time when traditional cell preparation techniques are used. For example, it is often necessary to change the preparation conditions, such as the sintering temperature, when using different electrolytes, so that the microstructure of the electrode could change with the electrolyte conductivity. This is the case with doped ceria electrolytes, for which the sintering temperatures are typically higher than corresponding temperatures for stabilized zirconia electrolytes. Indeed, Yamahara et al. recently expressed doubts whether the high ionic conductivities of the electrolyte materials used in composite electrodes are the dominant factor responsible for the comparative enhancements seen in cathode activity.[11] As pointed out earlier for SOFC anodes, enhanced performance with cathode composites prepared from doped ceria may be due to enhanced catalytic activity.[38–41]

In this study, infiltration methods were used to prepare the electrode composites because they offer a number of advantages relative to traditional fabrication methods.[42,43] First, the electrolyte scaffold is calcined separately at high temperatures, prior to the addition of the perovskite, so that there is good connectivity in the electrolyte phase and no solid-state reactions between the two phases of the composite. Furthermore, by using tape casting with the same pore formers, the structure of the electrolyte scaffold can be prepared for different electrolytes. In order to vary other materials properties of the electrolyte phase (e.g. surface energy, reducibility, chemical stability, activity as catalyst, etc.) as little as possible, we chose to

[*] Electrochemical Society Student Member.
[**] Electrochemical Society Active Member.
[z] E-mail: gorte@seas.upenn.edu

compare three zirconia-based materials with very different ionic conductivies: 8 mol % Y_2O_3-stabilized zirconia (YSZ), 10 mol % Sc_2O_3-stabilized zirconia (ScSZ), and 3 mol % Y_2O_3-20 mol % Al_2O_3-doped zirconia (YAZ).[44] We will demonstrate that the ionic conductivity of the electrolyte phase is very important in determining the cathode performance.

Experimental

Identical tape-casting procedures, described in more detail elsewhere,[10,42,43,45] were used to prepare porous-dense-porous structures from the three electrolyte materials. The three electrolytes that were used were 8 mol % yttria-stabilized zirconia (TZ-8Y, Tosoh), 10 mol % scandia-stabilised zirconia (Sc10SZ-TC, Fuel Cell Materials) or 20 mol % alumina, 3 mol % yttria co-doped zirconia (TZ-3Y20A, Tosoh). Tape-casting slurries for the dense layers were prepared by mixing 30 g of either YSZ, ScSZ, or YAZ with 13.5 g of distilled water, 0.8 g dispersant (D3005, Rohm & Haas), 5 g of binder HA12 (Rohm & Haas), and 6.5 g of binder B1000 (Rohm & Haas) in a beaker. Similarly, slurries for porous tapes were prepared by mixing 10 g of the ceramic material with 20 g of water 1.8 g of D3005, 4.8 g HA12, 7.2 g B1000, and 10 g of carbonaceous pore former (graphite, synthetic, <20 μm, Sigma Aldrich).

The green tapes were cut into the desired size and laminated into a porous-dense-porous YSZ trilayer structure. These structures were then fired to 1773 K for YSZ and ScSZ, and to 1823 K for YAZ for 4 h. For each of the trilayer structures, the porous layers were 50 μm in thickness and 65% porous, while the thicknesses of the dense layers were 100 μm for YSZ and ScSZ and 115 μm for YAZ. The diameter of the dense electrolytes was 1 cm, while the porous layers on opposite sides of the electrolyte were 0.67 cm in diameter.

All of the electrodes in the tested cells were produced by infiltration using aqueous nitrate solutions. For LSZ–YSZ, LSF–ScSZ, and LSF–YAZ symmetric cells, both of the porous scaffolds were infiltrated with an aqueous solution consisting of $La(NO_3)_3{\cdot}6H_2O$ (Alfa Aesar, 99.9%), $Sr(NO_3)_2$ (Alfa Aesar, 99%), and $Fe(NO_3)_3{\cdot}6H_2O$ (Fisher Scientific 98.4%) at a molar ratio of La:Sr:Fe = 0.8:0.2:1. Citric acid, in a 1:1 ratio with the metal cations, was used as a complexing agent to form the perovskite at lower temperatures. Each infiltration step was followed by heat treatment in air at 723 K. Multiple infiltration steps were needed to reach the final loading of 35 wt % (~20 vol %). In order to form the desired perovskite structure, the cells were heated in air to either 1123 or 1373 K for 4 h prior to applying Ag paste (SPI Supplies) for current collection.

To produce the fuel cells, the anode side was first infiltrated with a solution of $La(NO_3)_3{\cdot}6H_2O$, $Sr(NO_3)_2$, $Cr(NO_3)_3{\cdot}9H_2O$ (Acros Organics, 99%), $Mn(NO_3)_2{\cdot}6H_2O$ (Alfa Aesar, 99.98%), and citric acid at a molar ratio of La : Sr : Cr : Mn : citric acid = 0.8:0.2:0.5:0.5:2. Once a 45 wt % loading of $La_{0.8}Sr_{0.2}Cr_{0.5}Mn_{0.5}$ (LSCM) was achieved, the composite was fired to 1473 K for 4 h, followed by the infiltration of the LSF cathode. Finally, 5 wt % of CeO_2 (added as $Ce(NO_3)_3$, Alfa Aesar, 99.5%) and 0.5 wt % Pd (tetraamminepalladium (II) nitrate solution, Alfa Aesar, 99.9%) were added to the anode by infiltration for enhanced catalytic activity, followed by heat treatment at 723 K and the application of Ag current collector paste.

The fuel cells were attached to an alumina tube using a ceramic adhesive (Aremco, Ceramabond 552) so that the fuel (97% H_2-3% H_2O) could be introduced to the anode. Electrochemical impedance spectra were recorded using a Gamry Instruments potentiostat in the frequency range of 0.1 Hz–100 kHz. All symmetric cell impedances in this paper have been divided by two to account for there being two identical electrodes.

Results

SEM micrographs of the porous scaffolds prepared from each of the three electrolyte materials are shown in Fig. 1. The microstructure of the porous YSZ scaffold, Fig. 1a was in a good agreement with previous results from our laboratory.[10,43,45–47] The porosity

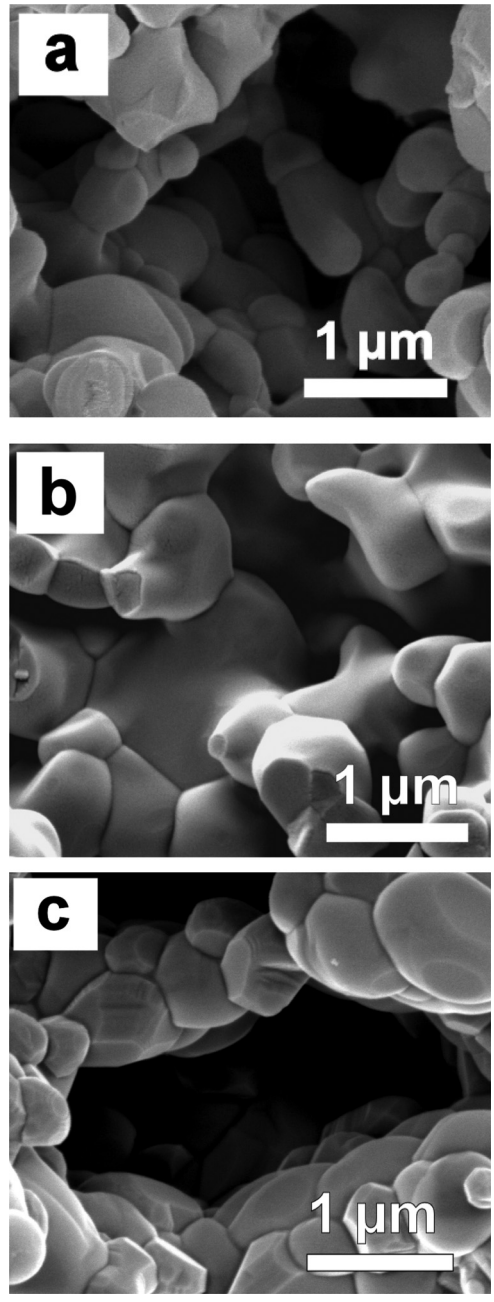

Figure 1. SEM images of porous stabilized zirconia scaffolds: (a) YSZ, (b) ScSZ, and (c) YAZ.

was 65%, as measured by the weight of water uptake, with the structure made up of ~1 μm pores.[47] Using the same recipe for the tape-casting procedure, porous scaffolds of ScSZ and YAZ, with very similar microstructures, were prepared. These are shown in Figs. 1b and 1c. Figures 2a through 2c show SEM of the same structures after infiltration of LSF with calcination to 1123 K. The composites are again nearly identical in appearance, with small LSF nanoparticles (~50 nm in diameter) deposited on the scaffold walls. After calcination to 1373 K, Figs. 2d through 2e, the LSF particles are no longer easily distinguishable from the electrolyte scaffold, appearing to form a dense film of LSF over the scaffolds. Qualitatively, there were no significant differences in the nature of the LSF particles in the three electrolyte scaffolds and the interactions between LSF and the three electrolyte materials were very similar.

Figure 3 shows i-V polarization curves measured at 973 K for fuel cells made from each of the electrolytes, operating on 97%

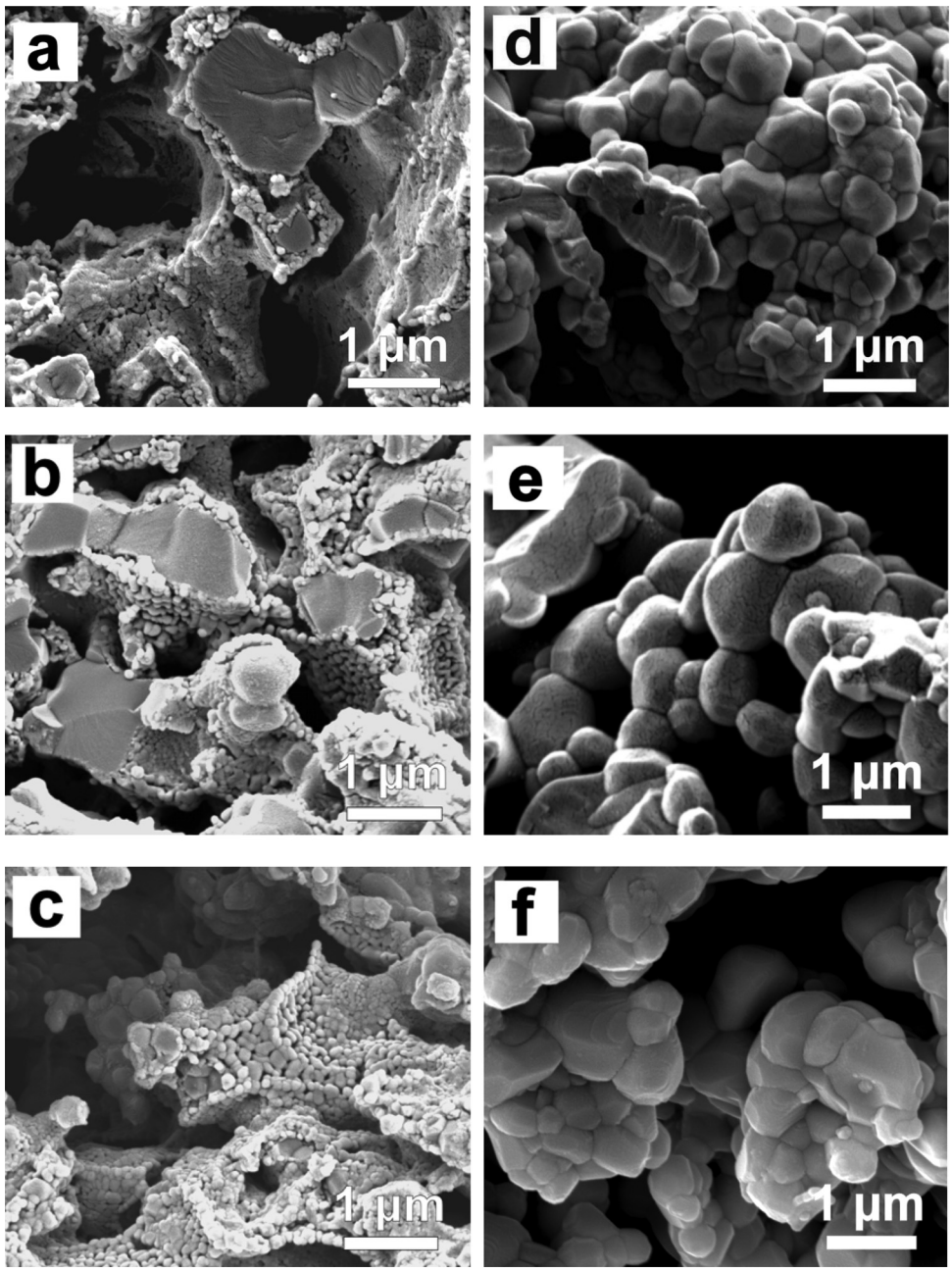

Figure 2. SEM images of porous 35 wt % LSF-SZ scaffolds: (a), (d) LSF-ScSZ, (b), (e) LSF-YSZ, and (c), (f) LSF-YAZ. Samples shown in (a), (b), and (c) were calcined to 1123 K, whereas samples (d), (e), and (f) were calcined to 1373 K.

H_2-3% H_2O at the anode and air at the cathode. The LSF composites in each of the cells had been calcined to 1123 K. The open circuit voltage (OCV) was above 1.05 V in each case, close to the Nernst Potential. However, the effect of electrolyte on the maximum power densities in these three cells is large, the YAZ cell exhibiting a maximum power density of 90 mW/cm^2, the YSZ cell 280 mW/cm^2, and the ScSZ cell 790 mW/cm^2. The i-V curves were also reasonably linear, implying that the impedance of cells was nearly independent of the applied load, so that impedance spectra measured at open circuit should provide a good measure of electrode performance. Based on the average slopes of i-V curves, the values of overall cell resistances were 0.36, 1.1, and 3.1 Ω cm^2 for cells based on ScSZ, YSZ, and YAZ, respectively.

The corresponding open-circuit impedance spectra for the three cells shown in Fig. 4, allow separation of the electrode and electrolyte losses. Based on the impedance spectra, the total cell resistances, determined from the zero-frequency intercept with the real axis in the spectra of Fig. 4, were 0.28 Ω cm^2 for the ScSZ cell, 0.84 Ω cm^2 for the YSZ cell, and 3.12 Ω cm^2 for the YAZ cell, in reasonable agreement with the average slopes determined from Fig. 3. The electrolyte losses, calculated from the high-frequency intercept with the real axis in the impedance spectra, were a large fraction of the losses in each cell. At 973 K, the ohmic contribution to the cells were 0.22 Ω cm^2 for the ScSZ cell, 0.51 Ω cm^2 for the YSZ cell, and 2.37 Ω cm^2 for the YAZ cell. When these losses are subtracted off from the total cell losses, the polarization losses associated with the electrodes is obtained, 0.06, 0.33, and 1.16 Ω cm^2 for LSF composites with ScSZ, YSZ, and (Y,Al)SZ, respectively. These data indicate that electrode losses depend strongly on the ionic conductivity of the electrolyte scaffold. However, because there are contributions from both the anode and cathode in these measurements, it is difficult to quantify the effect of the electrolyte from Fig. 4.

Since the ohmic contributions to the cell performance should not be affected by the electrodes, data like that in Fig. 4 can be used to measure the ionic conductivities of the three electrolytes and therefore provide a consistency check for the materials that we used. Therefore, impedance spectra were measured between 873 and 1073 K on each of the cells and the ohmic losses were used to calculate the

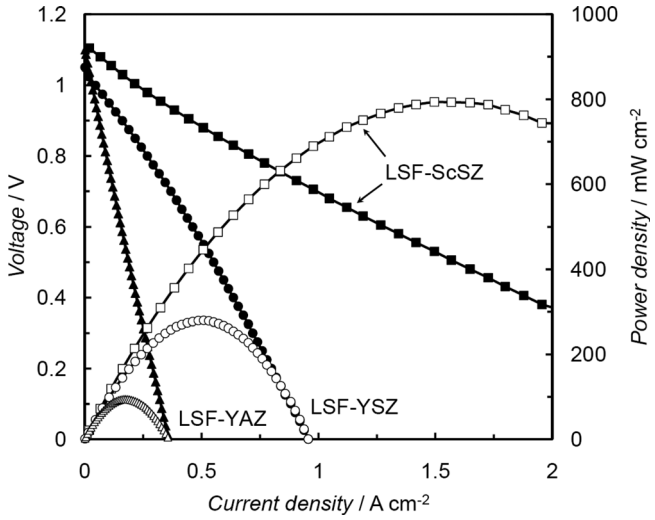

Figure 3. Polarization i-V curves for of LSF-SZ-LSCM, CeO_2, Pd fuel cell single cells with different electrolyte scaffolds after calcination to 1123 K, measured at 973 K. The cathode was subject to ambient air whereas 3% humidified H_2 was pumped onto the anode side. Closed symbols–voltage, open symbols–power density.

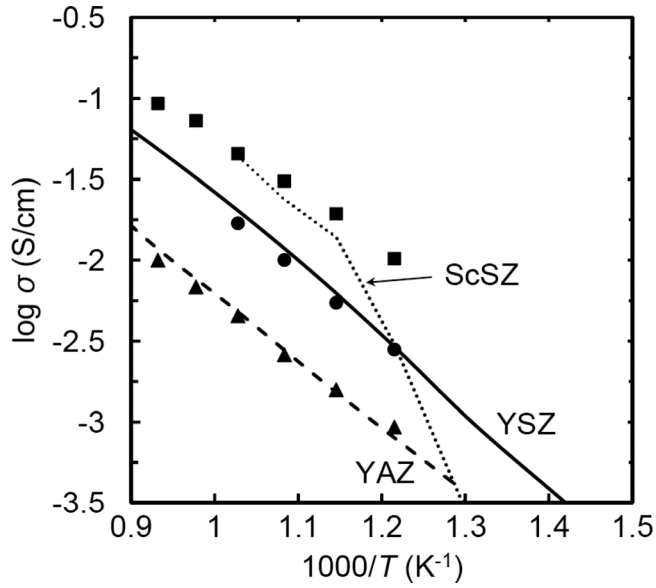

Figure 5. Comparison of experimental data (symbols), calculated from the high-frequency intercepts of fuel cell Cole-Cole plots, and literature values for the conductivity of the three electrolyte materials studied. References: ScSZ (Ref. 48); YSZ (Ref. 28), YAZ (Ref. 44).

ionic conductivities from the known electrolyte thicknesses. (The ionic conductivity, σ_i, is related to the ohmic resistance, R_Ω, and the thickness of the electrolyte, l, by $\sigma_i = l/R_\Omega$). The ionic conductivities determined from this are plotted in Fig. 5 along with literature data for each of the three electrolytes.[28,44,48] With the possible exception of the conductivity of ScSZ at 873 K, all of the experimental data agree with the literature values within the uncertainty of the measurements.

In order to isolate the effect of varying the electrolyte material on the electrochemical activity of the composite cathodes, symmetric cells were prepared in which LSF was infiltrated into both sides of the porous-dense-porous stabilized-zirconia structures. Impedance spectra were then measured in air over the temperature range from 873 to 973 K, the spectra obtained at 973 K shown in Fig. 6 for cells in which the LSF was calcined at 1123 K. The ohmic losses have been subtracted from the Cole-Cole plots and the values divided by two to account for the there being two electrodes. In agreement with the fuel cell data, the polarization resistances, R_p, increased with decreasing conductivity, with R_p being the smallest for ScSZ and the largest for YAZ. The values obtained from Fig. 6 for R_p at 973 K were 0.06 Ω cm^2 on the ScSZ cell, 0.14 Ω cm^2 on the YSZ cell, and 0.72 Ω cm^2 on the YAZ cell. These values are consistent with the impedances measured on the fuel cells in Fig. 3. Since the V-i polarization results in Fig. 3 indicated that the

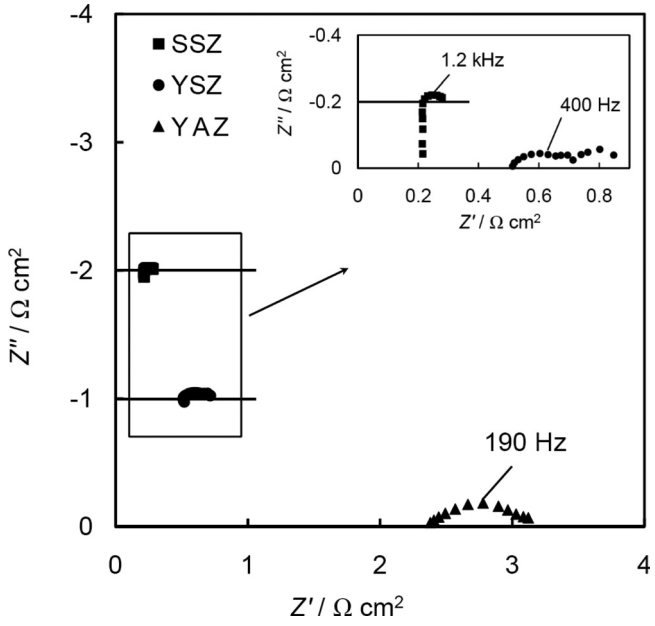

Figure 4. Electrochemical impedance spectra of LSF-SZ-LSCM,CeO_2,Pd fuel cell single cells with different electrolyte scaffolds after calcination to 1123 K, measured at 973 K in ambient air and open circuit conditions. Squares–ScSZ, circles–YSZ, triangles–YAZ.

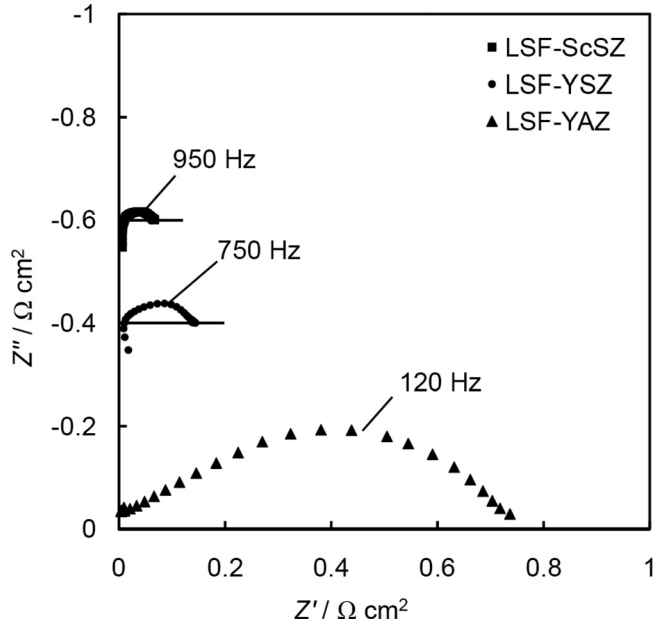

Figure 6. Electrochemical impedance spectra of LSF-SZ symmetric cells with different electrolyte scaffolds after calcination to 1123 K, measured at 973 K in ambient air and open circuit conditions. Squares–ScSZ, circles–YSZ, triangles–YAZ.

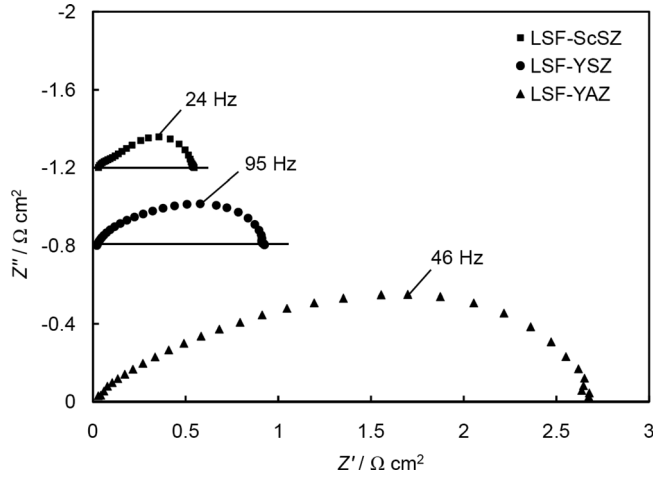

Figure 7. Electrochemical impedance spectra of symmetric cells with different electrolyte scaffolds after calcination to 1373 K, measured at 973 K in ambient air and open circuit conditions. Squares–ScSZ, circles–YSZ, triangles–YAZ.

impedances should be nearly independent of current, we also performed impedance measurements as a function of voltage on these cells and again found the results to be almost independent of the applied voltage over the range from −1 to 1 V.

Because the performance of infiltrated electrodes depends on the calcination temperature,[43,49,50] symmetric cells were also prepared with the LSF calcined to 1373 K for 4 h. Impedance spectra were again obtained in air from 873 to 973 K, with the spectra at 973 K shown in Fig. 7. Although the impedances on each of these cells were significantly higher, the relative performance as a function of the electrolyte was the same, with the ScSZ cell being the best with an R_p of 0.54 Ω cm^2, while the YSZ and YAZ cells showed significantly higher R_p of 0.91 and 2.67 Ω cm^2, respectively.

Two modeling studies have predicted that the polarization resistance of composite cathode should vary as the inverse square-root of the ionic conductivity of the electrolyte material.[3,37] Therefore, we have plotted the values of R_p that were obtained from the symmetric cells as a function of the ionic conductivity, with the results at 873, 923, and 973 K shown in Figs. 8a–8c. For the LSF cells calcined at 1373 K, the dependence of R_p on ionic conductivity was very close to the expected inverse square-root value. There does not seem to be a need to invoke other factors, such as differences in catalytic activity, to explain the relative performance of the cells made with these three electrolytes. However, for the LSF electrodes that were calcined at 1123 K, the electrode resistances varied with an almost inverse, first-order dependence on the ionic conductivity of the scaffold at each of the three temperatures. This result is perhaps biased by the poor performance of the cell made from YAZ. If factors in addition to ionic conductivity caused the performance of this cell to be worse, the dependence of R_p on ionic conductivity would be weaker. It is also possible that the electrode kinetics are not completely independent of the electrolyte material for cells heated to 1123 K.

It is interesting to consider the characteristic frequencies, ν_{char}, for the impedance data in Figs. 4, 6, and 7. For the cells calcined at 1123 K, ν_{char} increases in the order YAZ < YSZ < ScSZ. For example, for the fuel cell data shown in Fig. 4, the characteristic frequency of the YAZ cell was 190 Hz, while those of the YSZ and ScSZ cells were 400 Hz and 1.2 kHz, respectively. A similar trend can be seen in Fig. 6 for the corresponding symmetric cells. While the models, such as the Tanner-Virkar model[3] and the ALS model,[27] did not calculate the effect of the electrolyte conductivity on the characteristic frequency, Bidrawn, et al. did show that ν_{char} increased with decreasing R_p for electrodes with structures similar to those we have examined.[37] Although ν_{char} for cells calcined to 1373 K (Fig. 7) did not show a uniform trend with the ionic conductivity of the electrolyte, the strong current dependence of the electrode impedances after high-temperature calcination makes interpretation of these results more difficult.

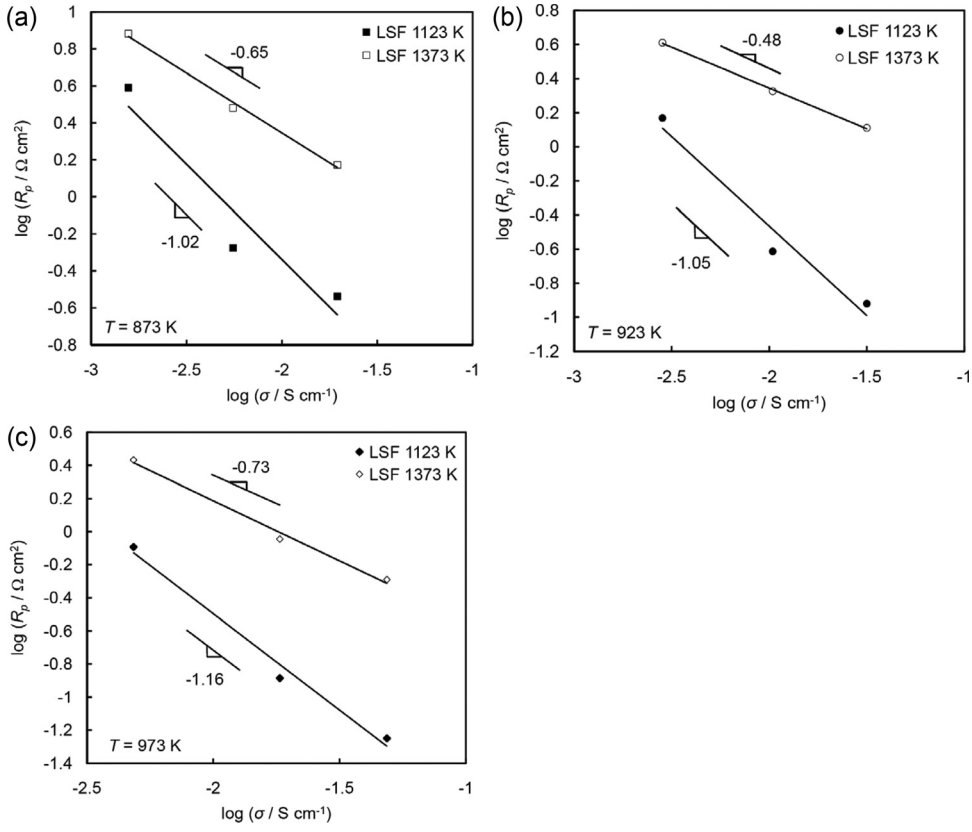

Figure 8. Log-log plot of the ionic conductivity of the electrolyte material vs the polarization resistance of the cathode symmetric cells calcined to either 1123 K (closed symbols) or 1373 K (open symbols) tested at open circuit conditions and at (a) 873 K, (b) 923 K, and (c) 973 K.

Discussion

The key finding of this study is that the ionic conductivity of the electrolyte used in composite cathodes has a large impact on the performance of these electrodes. More specifically, we have shown that the polarization resistance of composite electrodes decreases as the ionic conductivity of the electrolyte used in the composite increases, when all other materials properties (such as the catalytic activity, microstructure, reducibility, surface energy, etc.) are held constant. In contrast to doped ceria, none of the three electrolyte materials in this study is likely to possess significant activity towards oxygen reduction reaction, thus eliminating the possibility of electrode performance enhancement due to catalytic activity.

One implication of the finding that the performance scales with the ionic conductivity is that at least some of the enhancement observed when substituting YSZ with doped ceria in electrode composites arises from the increased ionic conductivity of the doped ceria. Of course, using a ceria-based composite can be advantageous in other ways. For example, doped ceria can prevent solid state reactions between YSZ and LSCo ($La_{1-x}Sr_xCoO_3$).[43,51–53] Ceria could also enhance performance through enhanced catalytic activity, since it is known to be a very good oxidation catalyst.[54,55]

Another implication of our results is related to low-temperature SOFCs. ScSZ is often proposed as a promising electrolyte material for anode-supported thin-electrolyte fuel cells operating at temperatures below 873 K.[12,56] The results of the present study demonstrate that a significant fraction of the enhanced performance of cells based on ScSZ could be due to enhanced performance of composite electrodes made from ScSZ. For very thin electrolytes, electrode losses frequently dominate. Improved ionic conductivity of the electrolyte within the composite electrodes could still affect the overall cell performance.

While all of the data in the present study was taken on composites of LSF and the electrolyte material, it is likely that the conclusions will be general for any perovskite so long as its ionic conductivity is less than that of the electrolyte. If electronically conductive materials could be found with ionic conductivities that were higher than that of the electrolyte, there would be no need for ionic conduction within the electrolyte phase. A corollary of this is that one should expect enhanced electrode performance following the addition of any material with high ionic conductivity to a composite cathode. Obviously, the structure of the composite is still important and one can only take advantage of a materials ionic conductivity if it is possible for that material to transport ions to the electrolyte.[49]

Conclusions

The performance of SOFC composite cathodes made from an electronically conductive perovskite and the electrolyte material is shown to depend on the ionic conductivity of the electrolyte. The dependence of the electrode resistance on the ionic conductivity of the electrolyte phase was found to be between to the power of -0.5 and -1. The results suggest that enhanced electrode performance can be achieved by incorporating a material with high ionic conductivity within composite electrodes.

Acknowledgment

This work was funded by the U.S. Department of Energy's Hydrogen Fuel Initiative (grant DE-FG02-05ER15721).

University of Pennsylvania assisted in meeting the publication costs of this article.

References

1. S. Singhal and K. Kendall, *High Temperature Solid Oxide Fuel Cells: Fundamentals, Design and Applications*, Elsevier Science, Oxford (2003).
2. N. G. Minh and T. Takahashi, *Science and Technology of Ceramic Fuel Cells*, Elsevier, Amsterdam (1995).
3. C. W. Tanner, K.-Z. Fung, and A. V. Virkar, *J. Electrochem. Soc.*, **144**, 21 (1997).
4. Y. Ji, J. A. Kilner, and M. F. Carolan, *Solid State Ionics*, **176**, 937 (2005).
5. T. Suzuki, M. Awano, P. Jasinski, V. Petrovsky, and H. U. Anderson, *Solid State Ionics*, **177**, 2071 (2006).
6. M. J. L. Østergård, C. Clausen, C. Bagger, and M. Mogensen, *Electrochim. Acta*, **40**, 1971 (1995).
7. M. J. Jørgensen, S. Primdahl, C. Bagger, and M. Mogensen, *Solid State Ionics*, **139**, 1 (2001).
8. M. J. Jørgensen and M. Mogensen, *J. Electrochem. Soc.*, **148**, A433 (2001).
9. J. Mertens, V. A. C. Haanappel, C. Wedershoven, and H.-P. Buchkremer, *J. Fuel Cell Sci. Technol.*, **3**, 415 (2006).
10. Y. Huang, K. Ahn, J. M. Vohs, and R. J. Gorte, *J. Electrochem. Soc.*, **151**, A1592 (2004).
11. K. Yamahara, T. Z. Sholklapper, C. P. Jacobson, S. J. Visco, and L. C. De Jonghe, *Solid State Ionics*, **176**, 1359 (2005).
12. K. Yamahara, C. P. Jacobson, S. J. Visco, and L. C. De Jonghe, *Solid State Ionics*, **176**, 275 (2005).
13. A. Selimovic, M. Kemm, T. Torisson, and M. Assadi, *J. Power Sources*, **145**, 463 (2005).
14. G. Anandakumar, N. Li, A. Verma, P. Singh, and J.-H. Kim, *J. Power Sources*, **195**, 6659 (2010).
15. E. Ivers-Tiffée, A. Weber, and D. Herbstritt, *J. Eur. Ceram. Soc.*, **21**, 1805 (2001).
16. S. P. Simner, J. F. Bonnett, N. L. Canfield, K. D. Meinhardt, J. P. Shelton, V. L. Sprenkle, and J. W. Stevenson, *J. Power Sources*, **113**, 1 (2003).
17. M. Søgaard, P. V. Hendriksen, and M. Mogensen, *J. Solid State Chem.*, **180**, 1489 (2007).
18. J. Mizusaki, M. Yoshihiro, S. Yamauchi, and K. Fueki, *J. Solid State Chem.*, **58**, 257 (1985).
19. Y. Huang, J. M. Vohs, and R. J. Gorte, *J. Electrochem. Soc.*, **151**, A646 (2004).
20. Z. Lu, J. Hardy, J. Templeton, and J. Stevenson, *J. Power Sources*, **196**, 39 (2011).
21. W. G. Wang and M. Mogensen, *Solid State Ionics*, **176**, 457 (2005).
22. A. Mai, V. A. C. Haanappel, S. Uhlenbruck, F. Tietz, and D. Stöver, *Solid State Ionics*, **176**, 1341 (2005).
23. S. P. Jiang, *Solid State Ionics*, **146**, 1 (2002).
24. J. M. Serra, V. B. Vert, M. Betz, V. A. C. Haanappel, W. A. Meulenberg, and F. Tietz, *J. Electrochem. Soc.*, **155**, B207 (2008).
25. M. Shah and S.A. Barnett, *Solid State Ionics*, **179**, 2059 (2008).
26. F. Bidrawn, S. Lee, J. M. Vohs, and R. J. Gorte, *J. Electrochem. Soc.*, **155**, B660 (2008).
27. S. B. Adler, J. A. Lane, and B. C. H. Steele, *J. Electrochem. Soc.*, **143**, 3554 (1996).
28. V. V. Kharton, F. M. B. Marques, and A. Atkinson, *Solid State Ionics*, **174**, 135 (2004).
29. A. Atkinson, S. Barnett, R. J. Gorte, J. T. S. Irvine, A. J. McEvoy, M. Mogensen, S. C. Singhal, and J. Vohs, *Nature Mater.*, **3**, 17 (2004).
30. H. Timmermann, D. Fouquet, A.Weber, E. Ivers-Tiffée, U. Hennings, and R. Reimert, *Fuel Cells*, **6**, 307 (2006).
31. M. Cimenti, V. Alzate-Restrepo, and J. M. Hill, *J. Power Sources*, **195**, 4002 (2010).
32. C. Lu, S. An, W. L. Worrell, J. M. Vohs, and R. J. Gorte, *Solid State Ionics*, **175**, 47 (2004).
33. H. Sumi, K. Ukai, Y. Mizutani, H. Mori, C.-J. Wen, H. Takahashi, and O. Yamamoto, *Solid State Ionics*, **174**, 151 (2004).
34. E. Perry Murray and S. A. Barnett, *Solid State Ionics*, **143**, 265 (2001).
35. K. Yamahara, C. P. Jacobson, S. J. Visco, X.-F. Zhang, and L. C. De Jonghe, *Solid State Ionics*, **176**, 275 (2005).
36. Z. Wang, M. Cheng, Y. Dong, M. Zhang, and H. Zhang, *Solid State Ionics*, **176**, 2555 (2005).
37. F. Bidrawn, R. Küngas, J. M. Vohs, and R. J. Gorte, *J. Electrochem. Soc.*, **158**, B514 (2011).
38. G. Zhou, P. R. Shah, T. Montini, P. Fornasiero, and R. J. Gorte, *Surf. Sci.*, **601**, 2512 (2007).
39. S. Hilaire, X. Wang, T. Luo, R. J. Gorte, and J. Wagner, *Appl. Catal., A*, **258**, 271 (2004).
40. J.-S. Kim, V. V. Nair, J. M. Vohs and R. J. Gorte, *Scr. Mater.*, (2010)
41. E. Aneggi, M. Boaro, C. de Leitenburg, G. Dolcetti, and A Trovarelli, *J. Alloys Compd.*, **408–412**, 1096 (2006).
42. J. M. Vohs and R. J. Gorte, *Adv. Mater.*, **21** 943 (2009).
43. R. Küngas, F. Bidrawn, J. M. Vohs, and R. J. Gorte, *Electrochem. Solid-State Lett.*, **13**, B87 (2010).
44. O. Yamamoto, T. Kawahara, K. Kohno, Y. Takeda, and N. Imanshi, in *Solid State Materials*, S. Radhakrishna and A. Daud, Editors, p. 372, Narosa Publishing House, New Delhi (1991).
45. M. Boaro, J. M. Vohs, and R. J. Gorte, *J. Am. Ceram. Soc.*, **86**, 395 (2003).
46. F. Bidrawn, S. Lee, J. M. Vohs, and R. J. Gorte, *J. Electrochem. Soc.*, **155**, B660 (2008).
47. H. Kim, C. da Rosa, M. Boaro, J. M. Vohs, and R. J. Gorte, *J. Am. Ceram. Soc.*, **85**, 1473 (2002).
48. J. H. Joo and G. M. Choi, *Solid State Ionics*, **179**, 1209 (2008).
49. F. Bidrawn, G. Kim, N. Aramrueang, J. M. Vohs, and R. J. Gorte, *J. Power Sources*, **195**, 720 (2010).
50. W. Wang, M. D. Gross, J. M. Vohs, and R. J. Gorte, *J. Electrochem. Soc.*, **154**, B439 (2007).
51. M. Shiono, K. Kobayashi, T. L. Nguyen, K. Hosoda, T. Kato, K. Ota, and M. Dokiya, *Solid State Ionics*, **170**, 1 (2004).
52. C. Rossignol, J. M. Ralph, J.-M. Bae, and J. T. Vaughey, *Solid State Ionics*, **175**, 59 (2004).
53. S. Uhlenbruck, T. Moskalewicz, N. Jordan, H.-J. Penkalla, and H. P. Buchkremer, *Solid State Ionics*, **180**, 418 (2009).
54. A. Trovarelli, *Catalysis by Ceria and Related Materials*, Imperial College, London (2002).
55. R. J. Gorte, *AIChE J.*, **56**, 1126 (2010).
56. T. Suzuki, Z. Hasan, Y. Funahashi, T. Yamaguchi, Y. Fujishiro, and M. Awano, *Science*, **325**, 852 (2009).